

Original scientific paper

**EVALUATION OF THE MAGNETIC FIELD GENERATED BY
A POWER CABLE IN PROXIMITY OF A JOINT BAY:
COMPARISON BETWEEN TWO DIFFERENT APPROACHES**

Giovanni Lucca

MERMEC STE Milano, Italy

Abstract. *The paper presents two different approaches for the evaluation of the magnetic flux density field produced by an underground power cable in proximity of areas where joint bays are present; as known, in those areas the field levels are generally much higher compared to the ones generated along the ordinary route. The first and more rigorous 3D approach takes into account the actual geometry of the power cable conductors in the joint bay, while the second one is based on a simplified 2D approach. The main result of the comparison is that the 2D approach, even at short lateral distances from the cable overestimates the field; therefore, one could adopt this method in order to rapidly and conservatively evaluate the distance of compliance (established by each specific national authority) from the cable in order to ensure protection of population from exposure to power frequency magnetic field.*

Key words: *magnetic field, power cables, human exposure to magnetic field, joint bay, Biot-Savart law, 3D and 2D method.*

1. INTRODUCTION

According to laws and regulations in many countries of the world, limits to protect general population and workers against exposure to 50-60Hz magnetic field have been established.

We may distinguish between limits to protect people against short-term exposure (that produces acute effects on human body) and limits to protect people against long-term exposure; by considering the latter issue and by following cautionary principles, many countries, have fixed limits, not to be exceeded, in places where continuative human presence is expected. It is worthwhile to mention that such limits are much lower (one or even two orders of magnitude) than the ones adopted for short-term exposure.

Received March 23, 2021; received in revised form May 6, 2021

Corresponding author: Giovanni Lucca

MERMEC STE, Via Stamira d'Ancona 9, 20127 Milano, Italy

E-mail: vanni_lucca@inwind.it

For example, ICNIRP (International Commission on Non-Ionizing Radiation Protection) [1], suggested the limit of $200\mu\text{T}$ (at the frequency of 50-60Hz) for population, but many single countries adopt, as a further cautionary measure against long-term effects, lower limits that are the order of few μT . Anyway, this paper shall neither cover any environmental or biological effects of magnetic field nor discuss any specific levels of magnetic field.

Thus, when a new power line has to be built, in order to accomplish the limits fixed by national regulations, one of the design steps consists in a preventive evaluation of the magnetic field generated by the line itself and in establishing a minimum distance from the power line axis in order to guarantee that, at any point beyond that distance, the magnetic flux density field does not exceed the limit fixed by the national regulations. We name such a distance Distance of Compliance and the acronym DOC will be used in the rest of the paper.

For example, in Italy, the limit of $3\mu\text{T}$ has been established by national law and thus the DOC is based on such a limit; the value of the DOC clearly depends on the characteristics and on the current carried by the power line.

Once the DOC has been evaluated, one can imagine to draw, along the power line route, a strip having half-width equal to the DOC. Inside this strip, no continuative human presence is allowed.

One has to bear in mind that the DOC may be not constant along the power line route because, when the conductors geometric disposition changes, the DOC varies as well.

An example of that, occurring when dealing with underground power cables, is represented by the joint bays.

We remind that the joint bays are located along the power cable route in those point where two different cable sections are joined together and, just in correspondence of them, the magnetic field produced by the cable is strongly increased compared to the the field level far from the joint bay itself.

That occurs because inside the joint bay, for technical reasons, the power cable conductors (phases) have to be arranged in flat disposition with an increase of the distance between them so producing a magnetic field that can be 5-10 times higher than the one produced by the same cable when the phases have trefoil configuration (typical disposition outside the joint bay).

A further point has to be mentioned: inside the joint bay the three phases of the cable change progressively their geometric arrangement because they widen out and go deeper (see a very simple sketch in Fig. 1) so that the invariance of phases disposition, along the cable route, is broken; this implies that the model of infinite conductors [2], or equivalently 2D model, normally adopted for calculating the magnetic field far from the joint bay is no more applicable and one has to use a more complex 3D model that takes into account of the varying distance among the conductors [3].

This does not imply that the simplified 2D model is useless: infact, the aim of this work is to show, by comparing the results obtained by means of the 3D and 2D models, that the latter one can be still adopted if our main purpose is to conservatively evaluate the DOC relevant to the power cable under study.

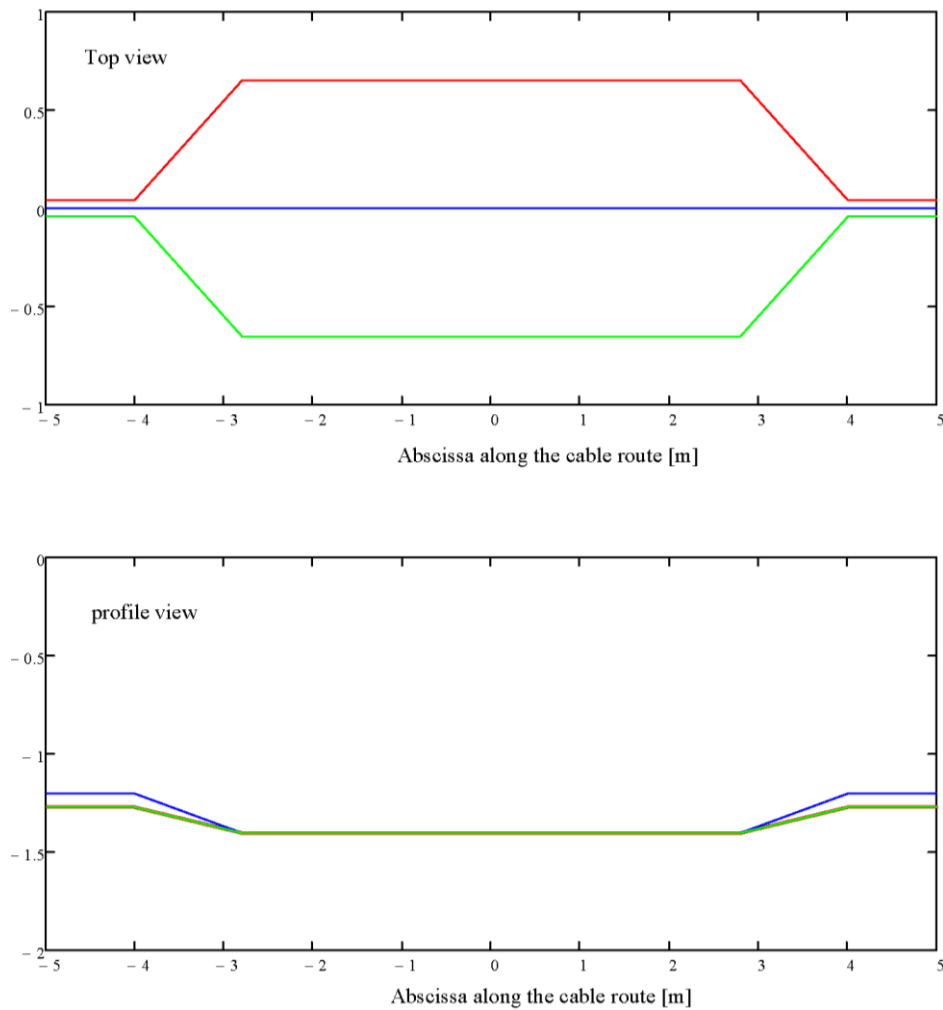


Fig. 1 Sketch (not in scale) of disposition of the conductors inside a joint bay

2. DESCRIPTION OF 3D MODEL

The 2D model is based on the well-known Biot-Savart law applied to infinitely long and rectilinear conductors; due to the fact that it is broadly described in literature, we omit any further detail about it. Information about this model can be found in [2].

On the contrary, it is useful to describe more in details the 3D model which, as mentioned before, allows for a correct evaluation of the magnetic flux density field when the geometry of the problem is more complex provided that the source of the field can be represented by a suitable number of straight wire segments carrying a known current.

This 3D model is still based on Biot-Savart law which is now applied to rectilinear conductor of finite length. (See for example [4-6]).

Thus, coming to our problem, if the power cable is composed by M conductors and each one of them is discretised by N wire segments, we have $N_{tot} = M \cdot N$ wire segments modelling the whole power cable.

Finally, if $B_{xk}(X, Y, Z)$, $B_{yk}(X, Y, Z)$, $B_{zk}(X, Y, Z)$ are respectively the x , y , z , components of the magnetic flux density field produced in the generic point of the space (X, Y, Z) by the k -th wire segment, the total magnetic flux density field is given by:

$$B_{xtot}(X, Y, Z) = \sum_{k=1}^{N_{tot}} B_{xk}(X, Y, Z) \quad (1)$$

$$B_{ytot}(X, Y, Z) = \sum_{k=1}^{N_{tot}} B_{yk}(X, Y, Z) \quad (2)$$

$$B_{ztot}(X, Y, Z) = \sum_{k=1}^{N_{tot}} B_{zk}(X, Y, Z) \quad (3)$$

and the modulus of the total field is:

$$|B_{tot}(X, Y, Z)| = \sqrt{|B_{xtot}(X, Y, Z)|^2 + |B_{ytot}(X, Y, Z)|^2 + |B_{ztot}(X, Y, Z)|^2} \quad (4)$$

Next step is to provide suitable analytical expressions for calculating the field produced by a single wire.

2.1. Field produced by a straight wire segment

Let us consider a generic straight wire having length S and carrying a constant current I (where I is a complex phasor); let us represent such a wire by means of an oriented segment with extremes in A and B of coordinates (x_A, y_A, z_A) and (x_B, y_B, z_B) respectively. By assuming the positive direction from A to B , we can define the relevant direction cosines l , m , n by:

$$\begin{pmatrix} l \\ m \\ n \end{pmatrix} = \begin{pmatrix} \frac{x_B - x_A}{S} \\ \frac{y_B - y_A}{S} \\ \frac{z_B - z_A}{S} \end{pmatrix} \quad (5)$$

Each point belonging to this segment can be represented by means of the following equations in parametric form:

$$\begin{pmatrix} x(s) \\ y(s) \\ z(s) \end{pmatrix} = \begin{pmatrix} x_A + ls \\ y_A + ms \\ z_A + ns \end{pmatrix} \quad (6)$$

The parameter s , appearing in (6), belongs to the interval $[0, S]$.

The starting point for the calculation of the magnetic flux density field produced by the wire conductor is given by the Ampere's law in differential form (see for example [7]) that expresses the field produced in a generic point (X, Y, Z) by a conductor having infinitesimal length dl and carrying a current I . (See Fig. 2)

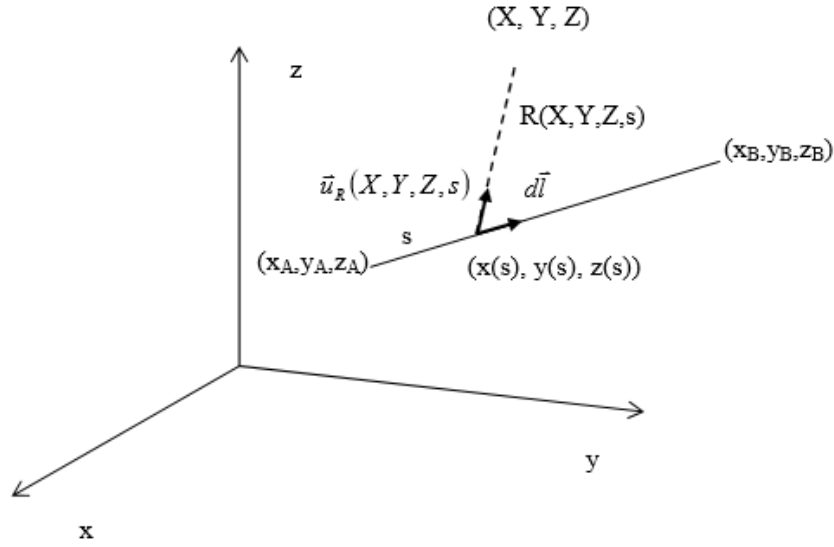


Fig. 2 Sketch of wire segment

This law is given by the formula:

$$d\vec{B}(X, Y, Z, s) = \frac{\mu_0 I d\vec{l} \times \vec{u}_r(X, Y, Z, s)}{4\pi R^2(X, Y, Z, s)} \quad (7)$$

where the distance $R(X, Y, Z, s)$ between the infinitesimal element dl and the point (X, Y, Z) is :

$$R(X, Y, Z, s) = \sqrt{(X - x(s))^2 + (Y - y(s))^2 + (Z - z(s))^2} \quad (8)$$

the vector $d\vec{l}$ is given by:

$$d\vec{l} = \begin{pmatrix} l ds \\ m ds \\ n ds \end{pmatrix} \quad (9)$$

the unit vector $\vec{u}_r(X, Y, Z, s)$ is expressed by:

$$\vec{u}_R(X, Y, Z, s) = \begin{pmatrix} \frac{X - x(s)}{R(X, Y, Z, s)} \\ \frac{Y - y(s)}{R(X, Y, Z, s)} \\ \frac{Z - z(s)}{R(X, Y, Z, s)} \end{pmatrix} \quad (10)$$

and μ_0 is the vacuum magnetic permeability.

The total field $\vec{B}(X, Y, Z)$ can be obtained by integrating (7) over the whole segment length; hence, by taking into account (8), (9), (10) one gets:

$$\vec{B}(X, Y, Z) = \int_0^s \frac{\mu_0 I (l\vec{u}_x + m\vec{u}_y + n\vec{u}_z) \times [(X - x(s))\vec{u}_x + (Y - y(s))\vec{u}_y + (Z - z(s))\vec{u}_z]}{4\pi \left(\sqrt{(X - x(s))^2 + (Y - y(s))^2 + Z - z(s))^2} \right)^3} ds \quad (11)$$

where $\vec{u}_x, \vec{u}_y, \vec{u}_z$ are respectively the unit vectors relevant to x, y, z axes.

By splitting up (11) into the three components, it is possible to analitically integrate each one of the three expressions (that we omit for brevity) so that one finally gets the following closed form expressions for the magnetic flux density field components:

$$B_x(X, Y, Z) = \frac{\mu_0 I [m(Z - z_A) - n(Y - y_A)]}{4\pi} \left\{ \frac{4S + 2K_1}{(4K_2 - K_1^2)\sqrt{S^2 + K_1S + K_2}} - \frac{2K_1}{(4K_2 - K_1^2)\sqrt{K_2}} \right\} \quad (12)$$

$$B_y(X, Y, Z) = \frac{\mu_0 I [-l(Z - z_A) + n(X - x_A)]}{4\pi} \left\{ \frac{4S + 2K_1}{(4K_2 - K_1^2)\sqrt{S^2 + K_1S + K_2}} - \frac{2K_1}{(4K_2 - K_1^2)\sqrt{K_2}} \right\} \quad (13)$$

$$B_z(X, Y, Z) = \frac{\mu_0 I [l(Y - y_A) - m(X - x_A)]}{4\pi} \left\{ \frac{4S + 2K_1}{(4K_2 - K_1^2)\sqrt{S^2 + K_1S + K_2}} - \frac{2K_1}{(4K_2 - K_1^2)\sqrt{K_2}} \right\} \quad (14)$$

being the quantities K_1 and K_2 given by:

$$K_1 = -2 [(X - x_A)l + (Y - y_A)m + (Z - z_A)n] \quad (15)$$

$$K_2 = (X - x_A)^2 + (Y - y_A)^2 + (Z - z_A)^2 \quad (16)$$

3. VALIDATION OF THE FORMULAS FOR 3D MODEL

Even if the 3D model based on the Biot-Savart law is broadly described in literature, it may be useful to compare the results obtained by applying the formulas presented in par.2 with the ones obtained by using some other very specific formulas, appearing in [8], that may serve as a benchmark. Such a benchmark is represented by the case of three parallel conductors of finite length carrying a tri-phase balanced current.

The three parallel conductors, carrying a current of 1000A, have length $L=10\text{m}$, lie on the x - z plane and are separated by a distance $d=0.3\text{m}$. The highest conductor has phase 240° , the lowest conductor has phase 120° and the middle conductor has phase 0° . (See Fig. 3)

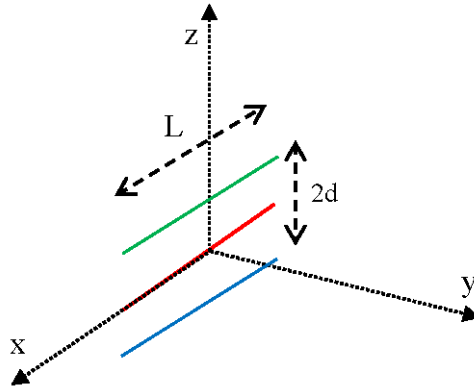


Fig. 3 Three conductors of finite length with vertical disposition

In Figs.4 the magnetic flux density field, calculated according to the two different formulations, is shown. In Fig. 4a, the field is evaluated along the x axis for different values of z ; conversely, in Fig. 4b, the field is evaluated along the y axis for different values of z . As one can see, in both the figures all the different couples of curves, corresponding to the same value of z , are superimposed.

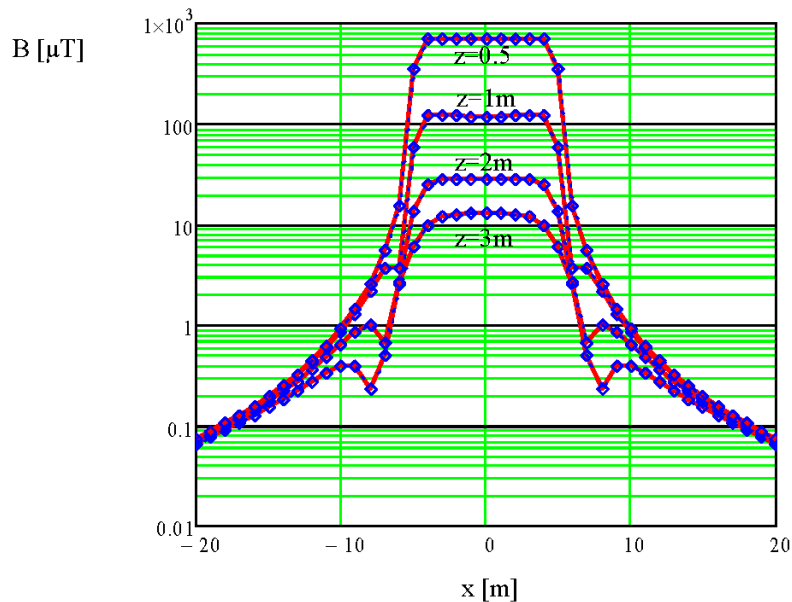


Fig. 4a Comparison of the B field; plot along the x axis for different values of z

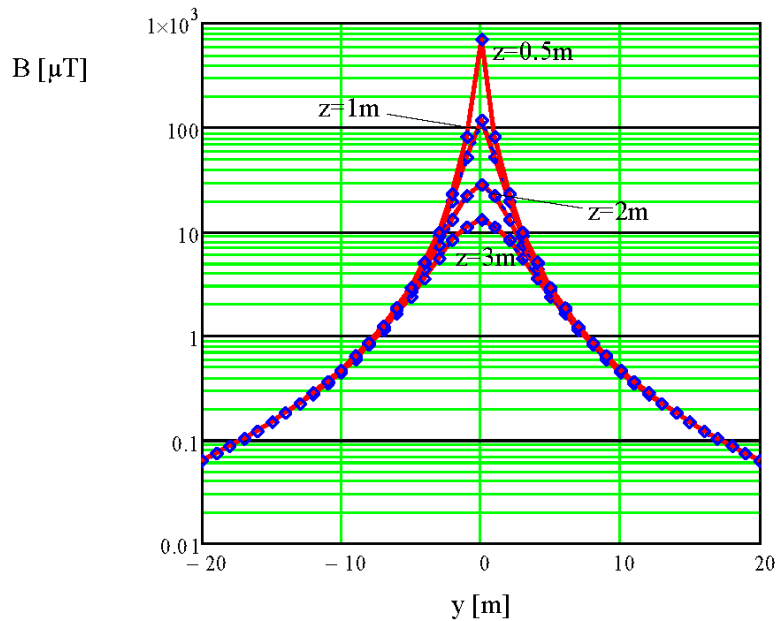


Fig. 4b Comparison of the B field; plot along the y axis for different values of z

4. COMPARISON BETWEEN THE TWO MODELS

Coming to the study of the joint bay, we shall consider two cases under the hypothesis that the power cable axis is parallel to the x-axis, while y is the lateral distance from the cable axis and z is the the quote/depth over/under the air-soil interface.

The first case deals with a single circuit power line while the second case deals with a double circuit power line.

In both the examples the power cables are carrying a balanced current of 1000A and the metallic sheaths of the phase conductors are supposed to be earthed in a single point so that no induced current can circulate on them. Anyway, the models can be easily adapted also to the case of solid bonding i.e.: the sheaths are earthed at least in two points so that induced currents can circulate on them thus generating a reduction of the magnetic field; see [2], [4], [9] for more details. In that case, the current I appearing in formulas (7) and from (11) to (14) represents the sum of the current flowing on the phase conductor with the one circulating on its own sheath. In particular, [2] and [4] give some indications on how to calculate the sheath current in a simplified way. Alternatively, the sheath current can be calculated, in a more precise way, by modelling the power cable as a multiconductor line; see [10], [11] for an exhaustive description of the multiconductor algorithm.

Lastly, the influence of the soil can be neglected because, at 50-60Hz and with balanced currents circulating on the phase conductors, the contribution given by it is very small. In fact, one could take into account of it by considering, for each conductor, a respective image current placed at a complex depth h_{im} given by [12-13]:

$$h_{im} = h + \frac{\sqrt{2}(1-j)}{2} \sqrt{\frac{\rho_s}{\omega\mu_0}} \quad (17)$$

Where h is the depth of the phase conductor, j is the imaginary unit, $\omega=2\pi f$ is the angular frequency and ρ_s is the soil resistivity; at 50-60Hz and for typical values of soil resistivity ($100\Omega\text{m}$ - $10000\Omega\text{m}$), one can immediately see that h_{im} is in the range from some hundreds of meters to some kilometers; thus, the image current of each conductor (that is related the soil effect) is so far away that has practically no influence on the value of the magnetic field evaluated at the distance of some meters from the cable.

4.1. Single circuit power line

We consider a power line section 160m long composed by one single tri-phase circuit having, just at the middle, a joint bay of length 8m so that its length is much less than the section length of power cable under study.

The conductors in the preceding and succeeding sections the joint bay have trefoil disposition while the arrangement of the conductors inside the joint bay is the one sketched in Fig. 1.

In Fig. 5 we show the magnetic flux density field evaluated along power cable axis at the air-soil interface by using the 2D and 3D models. In particular, we can notice the very fast increase/decrease of the field at the beginning/end of the joint bay where the conductors change their configuration from trefoil to flat and vice-versa.

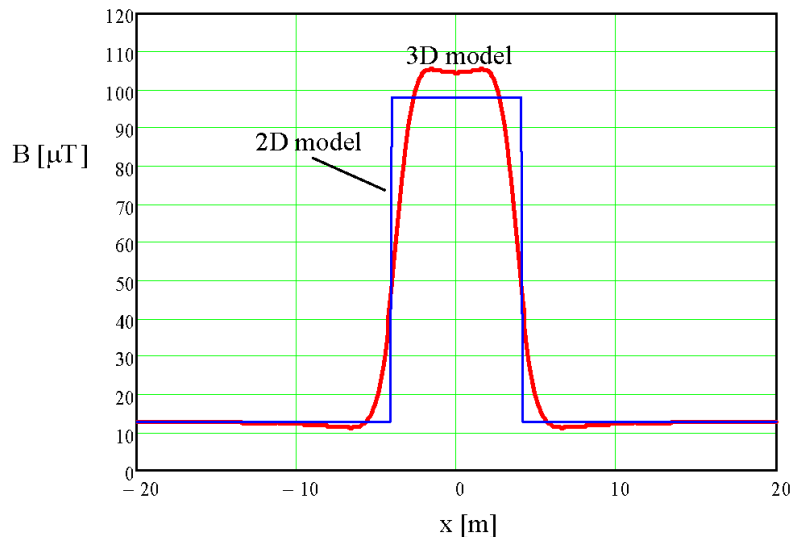


Fig. 5 B field along the power cable axis; $y=0$, $z=0$

In Fig. 6. we show the field evaluated at the middle of the joint bay ($x=0$) versus the lateral distance from the cable axis; the calculations are relevant to different heights from the soil.

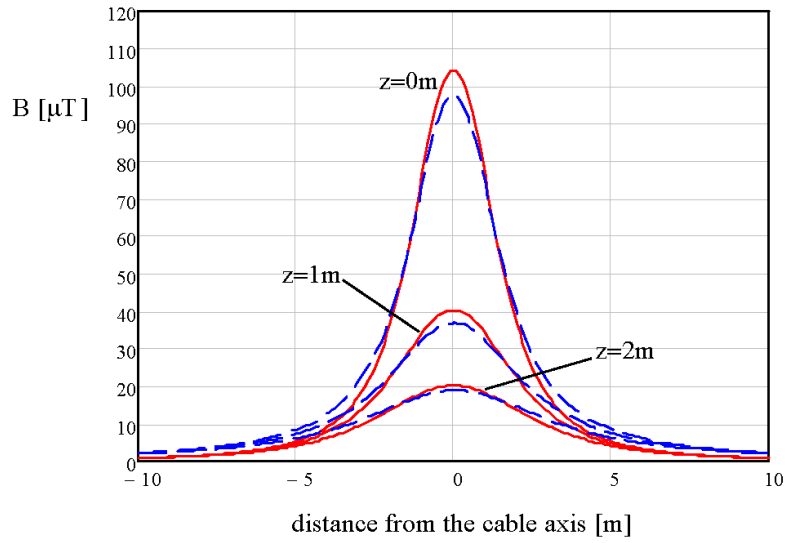


Fig. 6 B field versus lateral distance from power cable axis: continuous lines 3D model, dashed lines 2D model

In Fig. 7, starting from the results shown in Fig. 6, we plotted the percent relative error between the field calculated according to the 2D model and the 3D model respectively i.e.:

$$e_{\%}(x, y, z) = \frac{B_{3D}(x, y, z) - B_{2D}(y, z)}{B_{3D}(x, y, z)} 100 \quad (18)$$

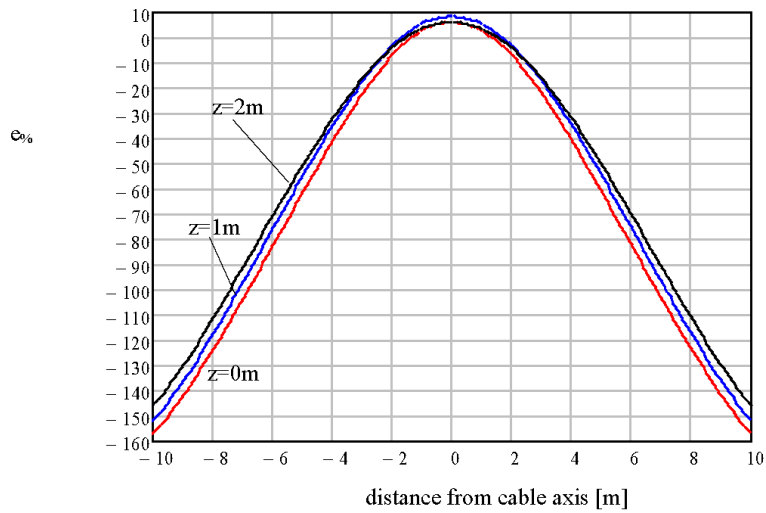


Fig. 7 Percent relative error versus lateral distance from power cable axis

From a look at Figs 5-7 it is evident that:

- Along the power cable route, the influence of the joint bay is restricted just to a short interval of few meters previous and next the joint bay itself.
- Inside and just outside the joint bay area, the fields calculated according to the two models are not very different (per cent relative error less than 10%) and the values obtained by 3D model are higher than 2D model.
- By increasing the lateral distance from the joint bay, the differences between the values obtained by the two models increase and we can notice that the 2D model overestimates the field.

4.2. Double circuit power line

We consider a power line section 160m long composed by a double tri-phase circuit having, just at the middle, a joint bay of length 19m so that the joint bay length is much less than the section length of power cable under study.

In this case, the geometry of the conductors inside the joint bay is more complicated because, for reasons of space, the two joints are staggered one respect to the other. See a sketch in Fig. 8

Like in the previous case, the conductors are disposed in trefoil configuration outside the joint bay.

The currents along the two circuits are disposed in order to minimize the field from a certain distance from the caviduct axis; i.e. the phases disposition is BAC-CAB [2]. The colors associated the phases are the same as in Fig. 3.

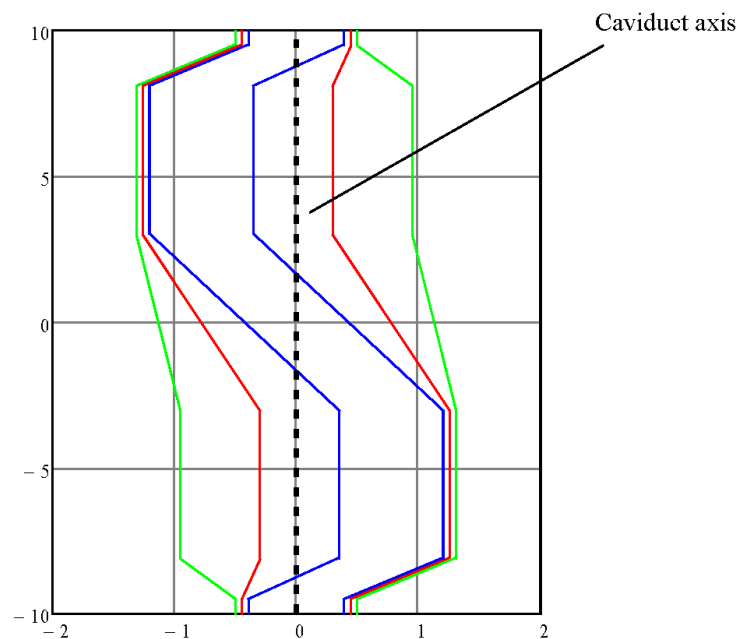


Fig. 8 Double circuit: sketch (not in scale) of the joint bay

We can notice that, in the first half of the joint bay, the conductors of the circuit on the left widen out while the conductors of the circuit on the right maintain their compact disposition; the reverse occurs in the second half of the joint bay.

In Fig. 9 we show the magnetic flux density field evaluated along the caviduct axis at the air-soil interface by using the 2D and 3D models.

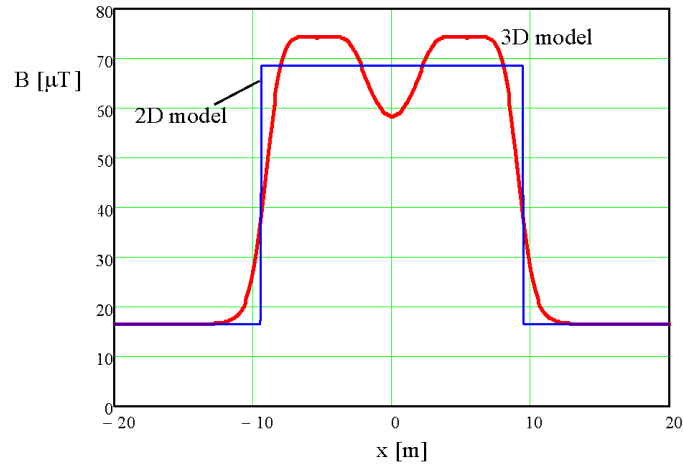


Fig. 9 B field along the caviduct axis; $y=0$, $z=0$

In Fig. 10 we show the field evaluated, according to the two models, at the middle of the left joint versus the lateral distance from the caviduct axis; the calculations are relevant to different heights from the soil. The results relevant to the right joint are exactly symmetrical with respect to the ones shown in Fig. 10; so, for brevity reasons, we omit them.

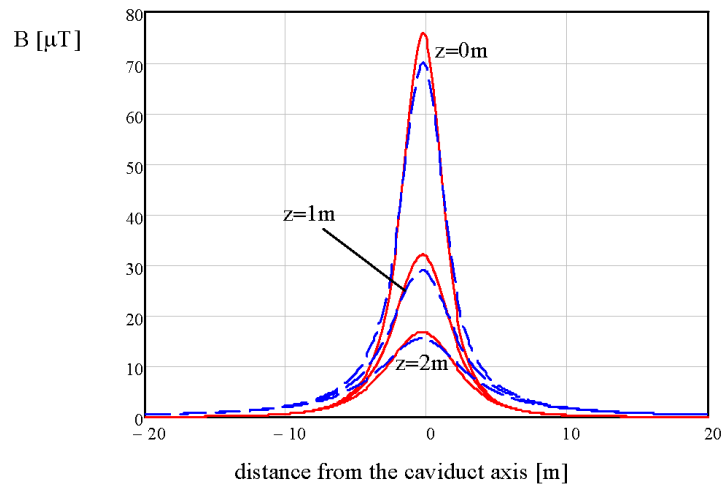


Fig. 10 B field versus lateral distance from caviduct axis: continuous lines 3D model, dashed lines 2D model

In Fig. 11, starting from the results shown in Fig. 10, we plotted the per cent relative error between the field calculated according to the 2D model and the 3D model respectively.

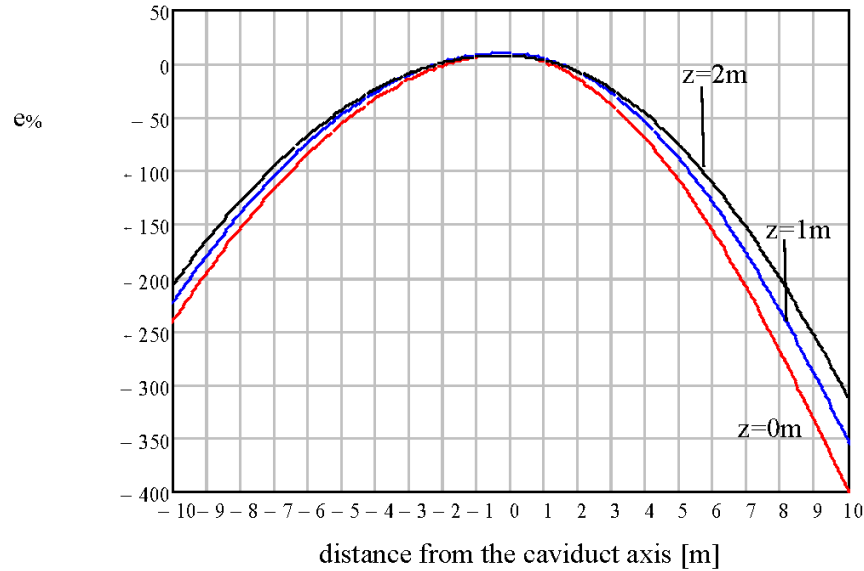


Fig. 11 Percent relative error versus lateral distance from caviduct axis

From a look at Figs 9-11 we can observe that the same remarks done for the single circuit still hold but with the difference that the discrepancies between the two models are more significative especially by moving away from the caviduct axis; compare Figs.7 and 11.

5. CONCLUSIONS

The basic conclusion we can draw from this study is that the 2D model allows for a conservative evaluation of the field outside the area occupied by the joint bay while, if an assessment of the field is needed in the area just over the joint bay, the 3D model has to be preferred even if the differences between the two models are not very large.

Therefore, we can summarize the outcome of our analysis by means the following remarks:

- 1) If the DOC around a joint bay has to be assessed, one can use the 2D model that it simpler and just needs the knowledge of the coordinates of the axis of the conductors when they are in flat disposition inside the joint bay.
The 2D approach could be adopted also for a simplified evaluation of the field in close proximity of the joint bay provided that the latter one is located far from areas where a continuative human presence is expected.
- 2) If the magnetic flux density field is aimed to a more precise evaluation, especially if mitigation measures are needed (such as shields, passive loops or other [14], [15]), then the use of the 3D model is necessary.

REFERENCES

- [1] ICNIRP, "ICNIRP Guidelines for limiting exposure to time varying electric and magnetic fields (1Hz-100kHz)", *Health Physics*, vol. 99, pp. 818-836, Dec. 2010.
- [2] CIGRE Joint Task Force 36.01/21, *Magnetic field in HV cable systems I/Systems without ferromagnetic component*. CIGRE, 1996, pp.1-5.
- [3] CIGRE, WG B1.23, TB 559, *Impact of EMF on current ratings and cable systems*. CIGRE 2013, pp.99.
- [4] Italian Standard CEI 211-4, *Guide to calculation methods of electric and magnetic fields generated by power-lines and electrical substations*, 2nd Edition, 2008, pp. 19-21. (In Italian).
- [5] K. J. Binn, P. J. Lawrenson and C. W. Trowbridge, *The Analytical and Numerical solution of Electromagnetic Fields*. John Wiley & Sons, 1992, pp. 76-79.
- [6] T. Modrić, S. Vujević and D. Lovrić, "3D Computation of the Power Lines Magnetic Field", *Prog. Electromagn. Res. M*, vol. 41, pp. 1-9, 2015.
- [7] E. C. Jordan and K. G. Balmain, *Electromagnetic Waves and Radiating Systems*. New Jersey: Prentice Hall, 1968, Chapter 3, pp. 86-88.
- [8] CIGRE, WG C4.204, TB 373, *Mitigation techniques of power-frequency magnetic fields originated from electric power systems*, *CIGRE*, 2009, pp. 18.
- [9] J. R. Riba Ruiz and X. Alabern Morera, "Effects of the circulating sheath currents in the magnetic field generated by an underground power line". In Proceedings of the International Conference on Renewable Energies and Power Quality ICREPQ'06, Palma de Mallorca, Spain, 5-7 April 2006, pp. 26-30.
- [10] ITU-T, *Directives concerning the protection of telecommunication lines against harmful effects from electric power and electrified railway lines*, ITU, vol. 3, Chapter 5, 1989.
- [11] C. R. Paul, *Analysis of Multiconductor Transmission Lines*. John Wiley & Sons, 1994, Chapter 4, pp. 186-246
- [12] ITU-T, *Directives concerning the protection of telecommunication lines against harmful effects from electric power and electrified railway lines*, ITU, vol. 2, 1999, p. 144
- [13] R. G. Olsen *et al.*, "Magnetic fields from electric power lines: theory and comparison to measurements", *IEEE Trans. Power Deliv.*, vol. 3, no. 4, pp. 2127-2136, Oct. 1988.
- [14] A. Canova and L. Giaccone "A novel technology for magnetic field mitigation: High Magnetic Coupling Passive Loops", *IEEE Trans. Power Deliv.*, vol. 26, no. 3, pp. 1625-1633, July 2011.
- [15] P. Maioli, "Shielding of electromagnetic field generated by HHV underground cable lines", In Proceedings of the 8th International Conference on Insulated Power Cables Jicable'11, Versailles, France, 19-23 June 2011.